Original Paper

phys. stat. sol. (a) **204**, No. 3, 737–744 (2007) / **DOI** 10.1002/pssa.200622287

Thermal characterization of ceramic tapes using photoacoustic effect

Annieta Philip K[*, **, 1], **Lyjo K. Joseph**[*, 1], **Litty M. Irimpan**[1], **Bindu Krishnan**[1, 2], **P. Radhakrishnan**[1], **V. P. N. Nampoori**[1], and **Raghu Natarajan**[2]

[1] International School of Photonics, Cochin University of Science and Technology, Kochi, Kerala 682022, India
[2] Centre for Materials for Electronics Technology (C-MET), Athani, P.O. Thrissur, Kerala, India

Received 9 June 2006, revised 18 October 2006, accepted 22 November 2006
Published online 16 January 2007

PACS 66.30.Xj, 78.20.Hp, 81.05.Je, 81.05.Qk

Thermal characterization of alumina–zirconia and zirconia ceramic tapes using a photoacoustic technique is presented. A transmission-mode geometry is employed for the measurement of thermal diffusivity while a reflection-mode geometry is used for the measurement of thermal effusivity. In both these geometries, the same open photoacoustic cell is used. From the measured values of thermal diffusivity and thermal effusivity, the thermal conductivity value has also been evaluated.

1 Introduction

Ceramics are considered to be one of the most suitable components for the fabrication of many of the devices used in the electronics and optoelectronics industries such as substrates for fiber-optic waveguides in integrated optics and components in microelectronics. In the case of ceramics, thermal accumulation causes thermally induced stresses in the sample, which in turn causes failure and deterioration in ceramic-based devices. Since ceramic tapes are used for microelectronic device fabrication, a thorough knowledge of the thermal parameters is essential. Even though ceramics are crystalline materials, like metals; they have little or essentially no electrical conductivity at room temperature because of fewer free electrons. They have high stability and, on an average, higher melting points and greater chemical resistance than metals and organic materials. The wear-resistance properties and high abrasion resistance behavior of the alumina–zirconia ceramic composites have been the focal point of many researchers [1]. This paper considers the thermal characterisation of alumina–zirconia and zirconia ceramic tapes using the photoacoustic (PA) method.

During the last decade, several methods have been developed for the nondestructive characterization of thermal, optical and structural properties of materials [2–9]. The laser-induced PA method has gained more popularity due to its simple, elegant experimental scheme as well as its versatility in employing different configurations to measure the required thermo-physical parameters with great accuracy [10–12]. The principle of the effect is that a sample in a closed cell illuminated by modulated light at audio frequencies produces an acoustic signal due to thermal waves resulting from nonradiative relaxation processes in the medium.

[*] Corresponding authors: e-mail: annietaphilip@yahoo.co.in, lyjokjoseph@yahoo.co.in, Phone: +91 484 2575848, Fax: +91 484 2576714
[**] Permanent address: The Cochin College, Kochi, Kerala, India

The PA technique has been made use of by many scientists for the measurement of thermal parameters of thin films and solid samples [13–22]. Since the phase shift of the signal does not depend on the optical properties of the sample, it is simpler to extract information on the thermal diffusivity (TD) from the experimental results.

2 Theoretical background

2.1 Thermal-diffusivity measurement

The temperature field in a homogeneous, linear-conducting solid in the absence of an internal heat source is described by the well-known equation,

$$\nabla^2 T = \frac{1}{\alpha}\frac{\partial T}{\partial t} \,. \tag{1}$$

The parameter α is the TD, given by

$$\alpha = \frac{k}{\rho C} \,, \tag{2}$$

where k is the thermal conductivity, ρ is the density and C is the specific heat capacity of the material. TD is an important thermophysical parameter, which essentially determines the diffusion of heat through a sample. The inverse of TD is a measure of time required to establish thermal equilibrium in a system for which a transient temperature change has occurred [23, 24].

The heat-transmission configuration is depicted in Fig. 1. For an optically opaque solid, the entire light is absorbed by the sample at $x = 0$ and the periodic heat is generated at the same place. Assuming that the heat flow into the air (ambient) in contact with the front surface of the solid is negligibly small, the thermal waves generated at $x = 0$ will penetrate through the sample to its rear surface. The heat thus reaching the sample-air interface at $x = -l_s$ will get attenuated after travelling a very small distance called the first thermal diffusion length in air. The thermal diffusion length is given by [5]

$$\mu = \left(\frac{2\alpha}{\omega}\right)^{\frac{1}{2}}, \tag{3}$$

where $\omega = 2\pi f$ and f is the modulation frequency of the incident light. Consequently, this periodic-heating process, arising as a result of the periodic absorption of light at the interface at $x = 0$, results in an acoustic piston effect in the air column in between the sample and the microphone.

According to the one-dimensional heat-flow model of Rosencwaig and Gersho [25, 26], for the arrangement schematically shown in Fig. 1, the pressure fluctuation in the air inside the chamber is given by [25–27],

$$Q = \frac{\gamma P_0 I_0 (\alpha_g \alpha_s)^{1/2}}{(2\pi)\, l_g T_0 k_s f \,\sinh(l_s \sigma_s)} \, e^{j(\omega t - \pi/2)} \,, \tag{4}$$

where γ is the ratio of specific heat capacities of air, P_0 and T_0 are the ambient pressure and temperature, I_0 is the radiation intensity, f is the modulation frequency, and l_i, k_i and α_i are the length, thermal conductivity and the TD of the medium. i = g, 0, s refers to the air, the ambient (air) and the solid sample,

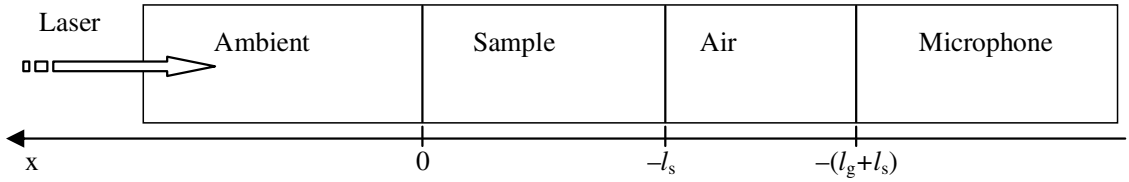

Fig. 1 Schematic representation of the open-cell geometry.

respectively. Also, $\sigma_i = (1 + j)\, a_i$ where $a_i = (\pi f/\alpha_i)^{1/2}$ is the thermal diffusion coefficient of the medium i. In arriving at the above expression it is assumed that the sample is optically opaque.

For a thermally thin sample (i.e. $l_s a_s \ll 1$), the expression for Q reduces to

$$Q = \frac{\gamma P_0 I_0 \alpha_g^{1/2} \alpha_s}{(2\pi)^{3/2} T_0 l_g l_s k_s} \frac{e^{j(\omega t - 3\pi/4)}}{f^{3/2}} . \tag{5}$$

The above expression implies that the PA signal (PAS) amplitude from a thermally thin sample under the heat-transmission configuration varies as $f^{-3/2}$ and the phase is insensitive to the variation in the modulation frequency.

When the sample is thermally thick (i.e. $l_s a_s \gg 1$), the expression for Q becomes

$$Q = \frac{\gamma P_0 I_0 (\alpha_g \alpha_s)^{1/2}}{\pi T_0 l_g k_s} \frac{\exp\left[-l_s (\pi f/\alpha_s)^{1/2}\right]}{f} e^{j(\omega t - \pi/2 - l_s a_s)} . \tag{6}$$

The amplitude of the PAS decreases with the modulation frequency as $(1/f)\exp\left(-b\sqrt{f}\right)$ with $b = l_s\sqrt{\pi/\alpha_s}$, while the phase ϕ decreases linearly with $b\sqrt{f}$. Hence, the TD (α_s) can be evaluated either from the amplitude data or from the phase data, provided the sample is optically opaque and thermally thick in the frequency region of interest. Although the phase and amplitude of the PAS contain a clear signature of the thermal properties of the specimen, phase data is more reliable for the open-cell configuration (OPC) since the amplitude data depends on many external parameters, such as sample surface quality and detector response at different wavelengths.

2.2 Thermal-effusivity measurement

Another useful thermal parameter, namely the thermal effusivity (TE), measures the thermal impedance of the material. It is the ability of the sample to exchange heat with the environment and hence it is an important parameter for surface heating and cooling processes. The major difference between TD and TE is that TD is a bulk property of the sample, whereas the TE is a surface property. The TE is defined as

$$e_s = k_s/\sqrt{\alpha_s} = \sqrt{k_s \rho C} . \tag{7}$$

The feasibility of the PA technique for the simultaneous measurement of thermal conductivity and heat capacity has already been established [28]. TE and thermal capacity values of ceramic tapes have great importance when they are used for microelectronic device fabrication or used as thermal barriers in integrated optics.

When the sample is kept in contact with a thermally thin absorbing layer, the acoustic pressure in the microphone chamber is given by the equation

$$\delta Q_1 = \frac{\gamma P_0 I_0 (\alpha_g \alpha_s)^{1/2}}{(2\pi)\, l_g T_0 k_s f} e^{j(\omega t - \pi/2)} , \tag{8}$$

where l_g is the length of the gas column in the cavity. The acoustic signal varies as $1/f$ and is proportional to the ratio $\sqrt{\alpha_s}/k_s$, the inverse of the TE of the sample.

In the absence of the sample (i.e. only the absorbing layer is present) the pressure fluctuation inside the cavity is given by

$$\delta Q_2 = \frac{\gamma P_0 I_0 \alpha_g^{1/2} \alpha_0}{(2\pi)^{3/2} T_0 l_g l_0 k_0} \frac{e^{j(\omega t - 3\pi/4)}}{f^{3/2}} . \tag{9}$$

The PAS varies as $f^{-3/2}$ and depends on the ratio α_0/k_0, so that we get

$$\frac{\delta Q_1}{\delta Q_2} \propto \frac{l_0 k_0}{\alpha_0} \frac{\sqrt{\alpha_s}}{k_s} f^{1/2} . \tag{10}$$

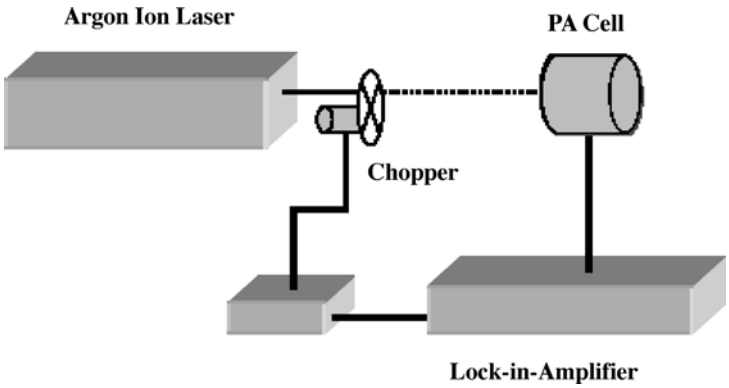

Fig. 2 Schematic diagram of the experimental setup.

This facilitates the normalization of the instrumental factor. The TE of the sample can be evaluated by measuring the signal amplitude as a function of the modulation frequency from the absorbing layer–sample composite and that from the absorbing layer alone, provided the thickness, density and specific heat capacity of the thin absorbing layer are known [29].

3 Experimental details

The experimental setup consists of an Argon ion laser (Liconix 5000 series, 488 nm, cw), a mechanical chopper (Stanford Research Systems SR540) and the OPC. The schematic of the experimental setup is given in Fig. 2. The OPC has provisions for both rear-side and front-side illumination.

The intensity-modulated optical radiation from the argon ion laser is allowed to fall on the sample kept inside the OPC. The PAS generated in the cell is detected using a sensitive electret microphone (Knowles BT 1834) and is amplified using a lockin amplifier. The phase and amplitude of the PAS are recorded using a digital lockin amplifier (Stanford Research Systems SR 830). Samples in the form of free-standing ceramic tapes are pasted on aluminum foils using thermal paste to avoid mechanical vibrations of the samples due to its periodic dilation (drum effect) during irradiation [19].

3.1 Sample specifications

The investigations were carried out on green ceramic tapes obtained from CMET, Thrissur. All the samples have a uniform thickness of 70 μm. The green tapes are prepared by the tape-casting technique [30] in which highly uniform ceramic sheets with no agglomeration or density gradient are obtained. These tapes have a polymer network in which ceramic particles are embedded uniformly [30, 31] and hence the heterogeneous (disordered system) treatment [32] is not considered. Therefore, no porosity is expected at the green stage. Only after the binder (polymer) burns out will porosity appear. The uniformity of green tapes is checked by cutting pieces from different portions of the tape and measuring the green density, which gives the same value. In the case of alumina–zirconia tapes, the utmost care is taken during the

Table 1 Sample specifications.

samples	% ceramic	% binder	% of plasticizer (phthalates and glycols)	% solvents
Al_2O_3/ZrO_2	36.41	21.5	3.33	38.76
ZrO_2	57.71	3.09	4.11	35.09

Note: In the case of Al_2O_3/ZrO_2 (alumina–zirconia) the solvent is water and the binder is polyvinyl alcohol (PVA) and for ZrO_2 the binder is polyvinyl butyral (PVB) and the solvent is water.

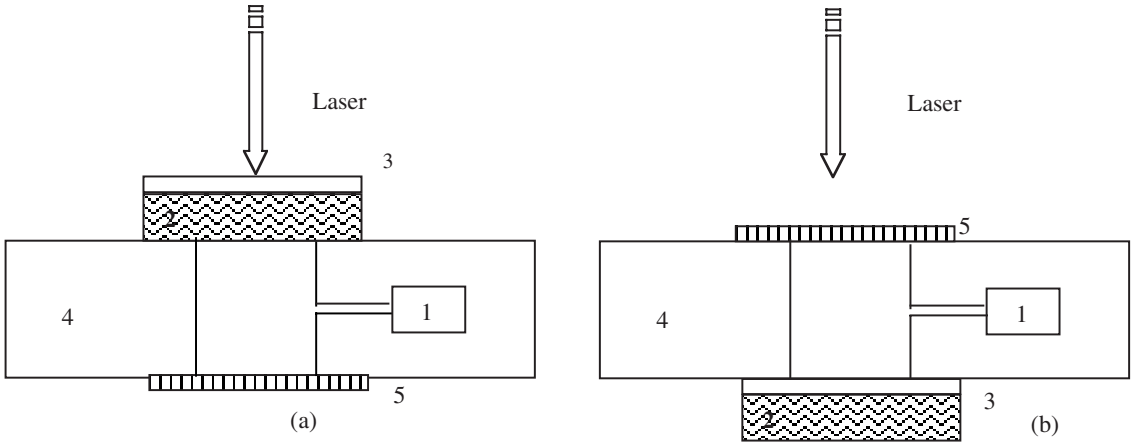

Fig. 3 Geometry for the measurement of (a) thermal diffusivity and (b) thermal effusivity. Cross-sectional view of OPC: 1 microphone, 2 sample, 3 aluminum foil, 4 acrylic body, 5 glass window.

preparation stages to adjust the pH and zetapotential of individual slurries before mixing to avoid both homo- and hetero-flocculation. Specifications of the samples are given in Table 1.

3.2 Thermal-diffusivity measurements

The rear-side illumination or the so-called heat-transmission configuration is used for the present investigations. The ceramic tape sample is pasted on thermally thin aluminum foil (5 μm thickness) using a thermal paste and is fixed to the top of the OPC using vacuum grease at the edges. The cell is arranged such that the modulated laser beam falls on the aluminum foil. The PAS phase is measured as a function of the modulation frequency. The same experiment is repeated with the aluminum foil alone. The difference in phase readings of the two observations gives the phase for the sample under investigation corresponding to different modulation values.

It may be noted that the one-layer treatment of PA is valid in this context as the thickness of the backing aluminum foil can be neglected since it conducts approximately the entire thermal signal through the foil.

3.3 Thermal-effusivity measurements

The same ceramic tape samples used in the experiment in reflection-mode geometry [33] and OPC were used for the TE measurements. The sample is pasted onto aluminum foil and the sample-aluminum foil combination is mounted on the PA cell so that the free surface of the sample faces the ambient. Irradiation is made through the front glass window and thermal waves are generated from the aluminum–gas interface.

4 Results and discussion

The variations of phase difference in the PAS (difference in the phases corresponding to the aluminum foil alone and the ceramic tape pasted on the aluminum foil) as a function of modulation frequency under the heat-transmission configuration for the samples under investigation are shown in Fig. 4.

The TDs of the samples are calculated from the slopes of the straight line graphs and are tabulated in Table 2. Literature values [34–38] of the TDs of pure ceramics and ceramic films are also included for comparison. Since tape casting is a batch process, there may be changes in the thermal parameters from batch to batch and these will depend on the presence of additives and binders, which are added during

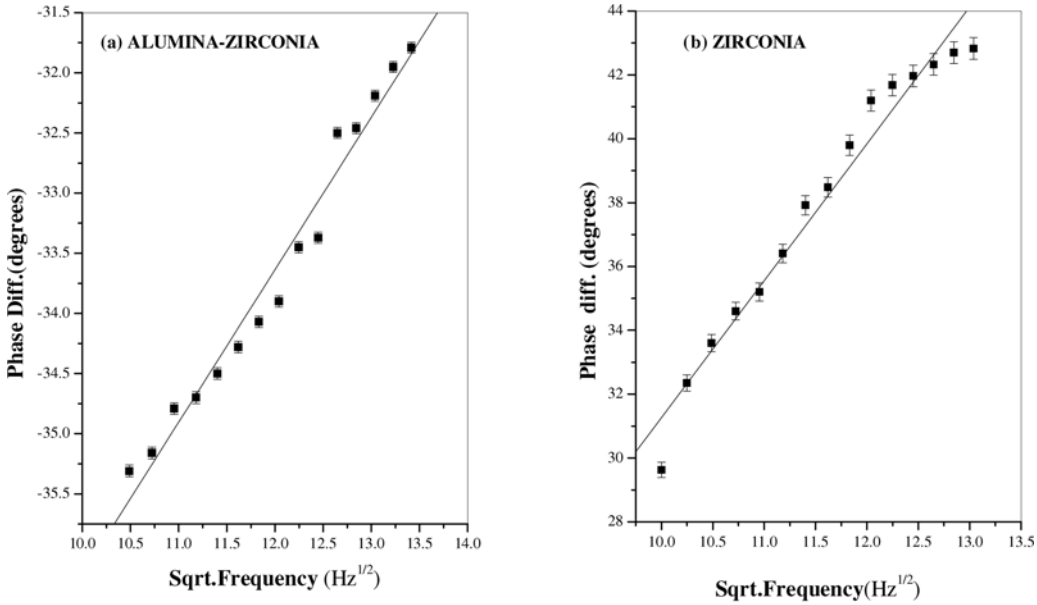

Fig. 4 Variations of PAS phase difference as a function of modulation frequency for (a) alumina–zirconia and (b) zirconia samples.

the tape-casting process. Values of thermal parameters of ceramic tapes are not available. However, it is seen from the table that the TD values calculated using the PA technique are of the same order of magnitude as that of the literature values of bulk materials. It is found that the presence of additives changes the TD of the compound. Alumina has a higher TD (~0.1 cm^2/s) [35, 38] compared to zirconia (~0.001 cm^2/s) [36]. The TD of the alumina–zirconia compound is greater than that corresponding to

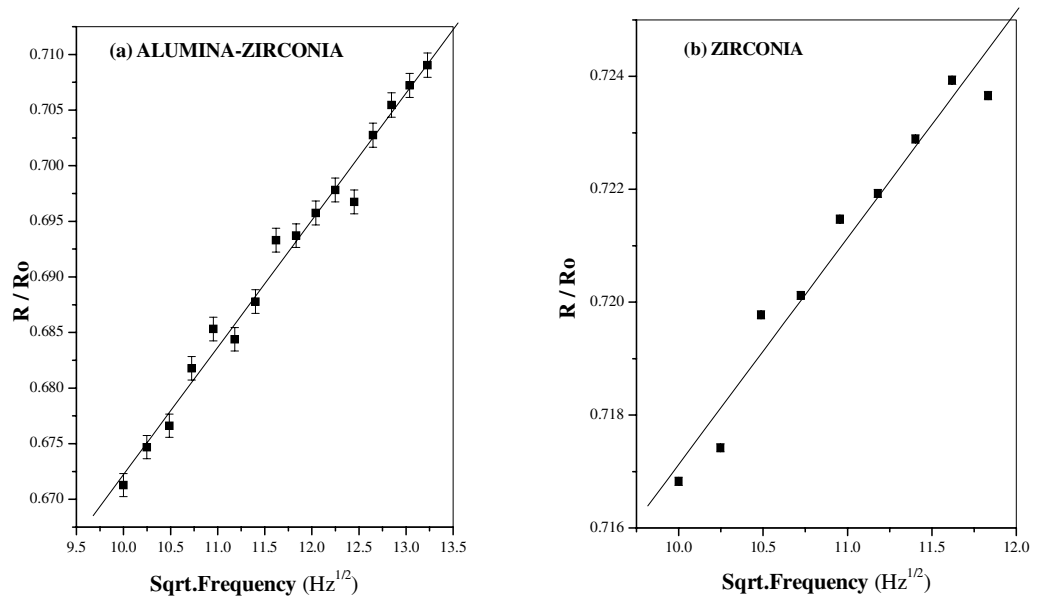

Fig. 5 Variation of ratio of PAS amplitude as a function of modulation frequency for (a) alumina–zirconia and (b) zirconia samples.

Table 2 Values of TD, TE and thermal conductivity values.

sample	TD ($cm^2\ s^{-1}$)	thermal conductivity ($W\ cm^{-1}\ K^{-1}$)	TE ($W\ s^{1/2}\ cm^{-2}\ K^{-1}$)	TD ($cm^2\ s^{-1}$) Refs. [34–37]
zirconia	0.0044 ± 0.0001	0.049 ± 0.001	0.74 ± 0.02	0.002–0.005
alumina–zirconia	0.0550 ± 0.0001	0.0610 ± 0.0001	0.260 ± 0.001	between 0.1 and 0.002

zirconia. Hence, the enhancement in thermal diffusion of the compound sample will be due to the presence of alumina. This shows that ceramic tapes with the required intermediate values of thermal parameters can be prepared by mixing appropriate amounts of different materials. The difference in the actual value can be attributed to the presence of materials other than ceramics.

Figure 5 shows the variation of the ratio of the PAS amplitude between the sample attached to the aluminum foil and the aluminum foil alone as a function of modulation frequency. The TEs are calculated from the slopes of the straight-line fits.

5 Conclusions

The present study clearly shows that the PA technique is an effective tool for the thermal characterization of ceramic samples. The details of investigations carried out on the thermal parameters of different ceramic (green) tape samples and the results obtained are presented. Analysis of results shows that the TD values depend on the constituents of the medium. Mixing one ceramic with another changes the effective thermal parameters of the sample. The deviation from the actual value of the TD of pure ceramics is attributed to the presence of materials other than ceramics.

Acknowledgements The authors LKJ and LMI are grateful to UGC (Government of India) for financial assistance. APK is thankful to the Cochin College, Kochi and BK acknowledges C-MET for the permission to pursue research work.

References

[1] L. N. Satapathy, Mater. Res. Bull. **34**, 1233 (1999) and the references therein.
[2] M. J. Adams, B. C. Beadle, G. F. Kirkbright, and K. R. Menon, Appl. Spectrosc. **32**, 430 (1978).
[3] C. A. Bennett and R. R. Patty, Appl. Opt. **20**, 911 (1981).
[4] G. Busse, Appl. Opt. **21**, 107 (1982).
[5] H. Coufal, P. Korpiun, P. Luscher, E. Schneider, and R. Tilgner, in: Photoacoustic Effect – Principles and Applications, edited by H. Coufal (Vieweg Verlag, Braunschweig, 1984).
[6] F. Lepoutre, G. Louis, and J. Taine, J. Chem. Phys. **70**, 2225 (1979).
[7] C. K. N. Patel and A. C. Tam, Appl. Phys. Lett. **36**, 7 (1980).
[8] A. C. Tam and H. Coufal, Appl. Phys. Lett. **42**, 33 (1983).
[9] R. R. Sanchez, J. B. Rieumont, S. L. Cardoso, M. G. da Silva, M. S. Sthel, M. S. O. Massunaga, C. N. Gatts, and H. Vargas, J. Braz. Chem. Soc. **10**, 97 (1999).
[10] A. Mandelis (ed.), Photoacoustic and Thermal Wave phenomena in semiconductors (North Holland, Amsterdam, 1987).
[11] H. Vargas and L. C. M. Miranda, Phys. Rep. **161**, 43 (1988).
[12] J. A. Balderas Lopez and A. Mandelis, J. Appl. Phys. **88**, 6815 (2000).
[13] M. J. Adams and G. F. Kirkbright, Anal. Chem. **51**, 508 (1979).
[14] D. M. Todorovic, P. M. Nikolic, D. G. Vaseljevic, and M. D. Dramicanin, J. Appl. Phys. **76**, 1 (1994).
[15] D. M. Todorovic and P. M. Nikolic, Proceedings of 20th International Conference on Microelectronics, Vol. 1 (MIEL'95) (NIS, Serbia, 1995).
[16] S. Sankararaman, V. P. N. Nampoori, C. P. G. Vallabhan, G. Ambadas, and S. Sugunan, Appl. Phys. Lett. **67**, 20 (1995).

[17] G. Gutierrez-Juarez, M. Vargas-Luna, J. J. Camacho-Espinosa, M. Sosa, J. L. Gonzalez-Solis, J. Bernal-Alvarado, and J. J. Alvarado-Gil, Rev. Sci. Instrum. **74**, 845 (2003).
[18] A. Bouguerra, A. Ledhem, J. P. Laurent, M. B. Diop, and M. Queneudec, J. Appl. Phys. **31**, 2184 (1998).
[19] A. M. Mansanares, H. Vargas, F. Galembeck, J. Buijs, and D. Bicanic, J. Appl. Phys. **70**, 7046 (1991).
[20] A. M. Mansanares, H. Vargas, A. C. Bento, N. F. Leite, and L. C. M. Miranda, Phys. Rev. B **42**, 4477 (1990).
[21] I. Deigadilio, A. Calderon, and L. C. M. Miranda, Opt. Eng. **36**, 343 (1997).
[22] G. Amato, G. Bendetto, L. Boarino, M. Maringelli, and R. Spagnoto, IEE Proc. A **139**, 4 (1992).
[23] M. Bertolotti, R. L. Votti, G. Liakhou, and C. Sibila, Rev. Sci. Instrum. **64**, 1576 (1993).
[24] S. D. George, P. Radhakrishnan, V. P. N. Nampoori, and C. P. G. Vallabhan, J. Phys. D, Appl. Phys. **36**, 990 (2003).
[25] A. Rosencwaig, Photoacoustics and Photoacoustic Spectroscopy (John Wiley & Sons, New York, 1980).
[26] A. Rosencwaig and A. Gersho, J. Appl. Phys. **47**, 64 (1976).
[27] L. F. Perondi and L. C. M. Miranda, J. Appl. Phys. **62**, 2955 (1987).
[28] U. Zammit, M. Marinelly, R. Pizzoferrato, F. Scudieri, and S. Martelluci, J. Phys. E, Sci. Instrum. **21**, 935 (1988).
[29] Nibu A. George, C. P. G. Vallabhan, V. P. N. Nampoori, A. K. George, and P. Radhakrishnan, Opt. Eng. **40**, 1343 (2001).
[30] K. P. Plueknett, C. H. Caeeres, and D. S. Willinson, J. Am. Ceram. Soc. **77**, 2137 (1991).
[31] E. M. Deliso, W. R. Cannon, and A. S. Rao, Adv. Ceram. **24**, 335 (1988).
[32] L. J. Inglehart, A. Broniatowski, D. Fournier, A. C. Boccara, and F. Lepoutre, Appl. Phys. Lett. **56**, 1749 (1990).
[33] L. Veleva, S. A. Tomas, E. Marin, A. Cruz-Orea, I. Delgadillo, J. J. Alvarado-Gil, P. Quintana, R. Pomes, F. Sanchez, H. Vargas, and L. C. M. Miranda, Corros. Sci. **39**, 1641 (1997).
[34] P. Charpentier, F. Lepoutre, and L. Bertrand, J. Appl. Phys. **53**, 608 (1982).
[35] Mitsue Ogawa, Kazuo Mukai, Takehisa Fukui, and Tetsuya Baba, Meas. Sci. Technol. **12**, 2058 (2001).
[36] National Physical Lab. TPAC News 7.
[37] N. P. Bansal and D. Zhu, NASA /TM 212896 (2003).
[38] Atsumasa Yoshida, Hideo Nogami, Takahiro Kurita, and Seiichi Washio, Anal. Sci. **17**, 154 (2001).

